Optical and Quantum Electronics **32:** 885–897, 2000.

Analysis of nonreciprocal light propagation in multimode imaging devices

O. ZHUROMSKYY[1], M. LOHMEYER[1], N. BAHLMANN[1], P. HERTEL[1], H. DÖTSCH[1] AND A.F. POPKOV[2]
[1]*Department of Physics, University of Osnabrück, Barbarastraße 7, D-49069, Germany (E-mail: azhuroms@uos.de)*
[2]*Zelenograd Research Institute of Physical Problems, 103460 Moscow, Russia*

Abstract. We investigate a structure consisting of a magneto-optic multimode waveguide and two monomode waveguides serving as in- and outlets. The geometrical dimensions of the multimode waveguide can be adjusted such that the guided modes interfere constructively in forward direction and destructively for backward propagation. In this paper we present concepts for a circulator and two isolators based on multimode imaging.

Key words: integrated optics, magneto-optics, multimode imaging, optical isolator

1. Introduction

In recent years quite a few concepts of integrated optical isolators and circulators were presented (Yamamoto *et al.* 1976; Ando *et al.* 1988; Hemme *et al.* 1990; Wolfe *et al.* 1990; Shintaku 1995). Most of them rely on complex structures such as Mach–Zehnder interferometers (Auracher *et al.* 1975; Okamura *et al.* 1984; Bahlmann *et al.* 1998; Zhuromskyy *et al.* 1999) or radiatively coupled waveguides (Lohmeyer *et al.* 1998, 1999; Bahlmann *et al.* 1999) which are difficult to realize because of the complexity of the structures and due to strict tolerance requirements. In this paper, we propose new designs of integrated optical isolators and circulators based on multimode imaging which are less complicated.

Today multimode-interference-based devices are used as couplers and recombiners (Jenkins *et al.* 1994; Soldano *et al.* 1995), power splitters, or combiners in ring lasers (Krauss *et al.* 1995). Modes of the multimode waveguide excited by incoming light form an image at a distance L from the beginning of the multimode segment, where the phases satisfy $\varphi^{\nu}(L) = \varphi^{\nu}(0) + 2\pi n^{\nu}$ for all guided modes ν of the multimode waveguide, n^{ν} are integers. The distance L depends strongly on the wavenumbers (propagation constants) β^{ν} of the guided modes. In magneto-optic waveguides, a magnetization oriented perpendicular to the direction of light propagation causes wavenumbers of counterpropagating modes to be different. In this

case, the distance between two images differs for forward and backward propagation. It is possible to adjust the length of the multimode waveguide such that there is constructive interference in forward and destructive interference in backward direction. The magnetization pattern of the multimode waveguide influences the length of the device. We have employed the wave-matching method (Lohmeyer 1997, 1998) for accurate calculations of guided modes. The nonreciprocal effects are treated in the framework of perturbation theory.

2. Nonreciprocal phase shifters

We refer to a structure as sketched in Fig. 1. Light propagates along the z direction, x and y denote the transverse coordinate axes with the y axis parallel to the substrate. In magneto-optic waveguides, with magnetization perpendicular to the direction of light propagation, the mode wavenumbers differ for forward and backward propagation (Wallenhorst *et al.* 1995; Popkov *et al.* 1998). Since magneto-optic effects are weak, perturbation theory can be used to estimate the shift $\delta\beta$ of the mode wavenumber due to gyrotropy, and the mode wavenumber β can be calculated as

$$\beta = \beta_0 + \delta\beta, \tag{1}$$

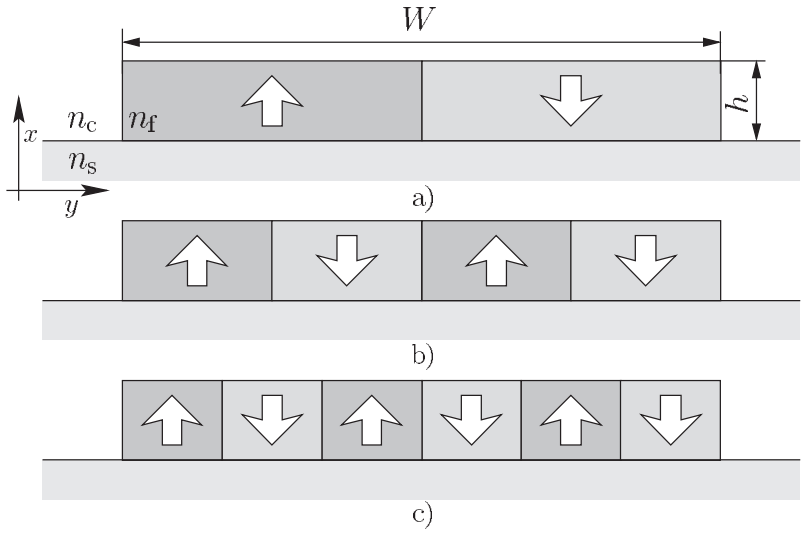

Fig. 1. Nonreciprocal phase shifters for TE modes: (a) two domain, (b) four domain, (c) six domain structures. x and y denote the transverse coordinate axes, the propagation axis z is normal to the figure plane. n_f, n_c and n_s are the refractive indices of the film, cover, and substrate respectively. Arrows indicate the sign of the intrinsic Faraday rotation.

where β_0 is the mode wavenumber without gyrotropy. The permittivity tensor of a medium magnetized along the x direction can be written in the form

$$\hat{\varepsilon} = \begin{pmatrix} \varepsilon & 0 & 0 \\ 0 & \varepsilon & 0 \\ 0 & 0 & \varepsilon \end{pmatrix} + \begin{pmatrix} 0 & 0 & 0 \\ 0 & 0 & -\mathrm{i}\gamma_\mathrm{x} \\ 0 & \mathrm{i}\gamma_\mathrm{x} & 0 \end{pmatrix}, \tag{2}$$

where the first term represents permittivity without magnetization and the second term is the magneto-optic contribution to the permittivity tensor, index x indicating the direction of magnetization. The off diagonal element γ is related to the specific Faraday rotation Θ_F and vacuum wavelength λ by $\gamma = n\lambda\Theta_\mathrm{F}/\pi$ where n is the refractive index of the medium. The shift of the mode wavenumber by the magneto-optic effect can be calculated from the fields $(\boldsymbol{E}, \boldsymbol{H})\exp(\mathrm{i}(\omega t - \beta_0 z))$ of the unperturbed system as follows (Popkov *et al*. 1998)

$$\delta\beta = \frac{\omega\varepsilon_0}{N}\iint (\boldsymbol{E}^* \Delta\hat{\varepsilon}\boldsymbol{E})\mathrm{d}x\,\mathrm{d}y, \tag{3}$$

where ω denotes the angular frequency of light, ε_0 is the vacuum dielectric susceptibility, $\Delta\hat{\varepsilon}$ represents the second term in the right-hand side of expression (2), and the normalization coefficient N equals

$$N = \iint [\boldsymbol{E} \times \boldsymbol{H}^* + \boldsymbol{E}^* \times \boldsymbol{H}]_\mathrm{z}\,\mathrm{d}x\,\mathrm{d}y. \tag{4}$$

We shall discuss TE modes because the output of integrated optical lasers is usually TE polarized. All considerations (apart from the nonreciprocal phase shift calculations) are applicable to the case of TM-polarized light as well.

The phase shift for a TE mode is given by the expression

$$\delta\beta_\mathrm{TE} = \frac{\omega\varepsilon_0}{\beta N}\iint \gamma_\mathrm{x}\partial_\mathrm{y}|E_\mathrm{y}|^2\mathrm{d}x\,\mathrm{d}y. \tag{5}$$

Taking into account the symmetry of the modes we can see that the integral in expression (5) is nonzero only if γ_x is asymmetric with respect to the xz-plane. Fig. 1 shows phase shifters for TE modes. Changing the direction of light propagation amounts to changing the sign of γ. Using (5) we may write

$$\delta\beta_{\mathrm{b}} = -\delta\beta_{\mathrm{f}}, \tag{6}$$

where the suffixes 'f' and 'b' represent the forward and backward direction of light propagation. Fig. 2 presents nonreciprocal phase shifts of mode wavenumbers in structures depicted in Fig. 1. The differences in the nonreciprocal phase shifts can be explained as follows. Expression (5) may be rewritten in the form

$$\delta\beta_{\mathrm{TE}} = \frac{\omega\varepsilon_0}{\beta N}\sum_n \left(\int \gamma_{\mathrm{x}} |E_{\mathrm{y}}|^2 \, \mathrm{d}x \Big|_{\Gamma_n - 0} - \int \gamma_{\mathrm{x}} |E_{\mathrm{y}}|^2 \, \mathrm{d}x \Big|_{\Gamma_n + 0} \right), \tag{7}$$

where Γ_n are lines of discontinuities of γ_{x} and $n = 0, 1..$ indicates the number of the interface. In the case of a two-domain structure, for example, three interfaces give rise to a nonreciprocal phase shift. The contribution from the strip sidewalls is small because the fields are weak there. We obtain a large contribution from the central discontinuity for all symmetric modes and no phase shift for antisymmetric modes.

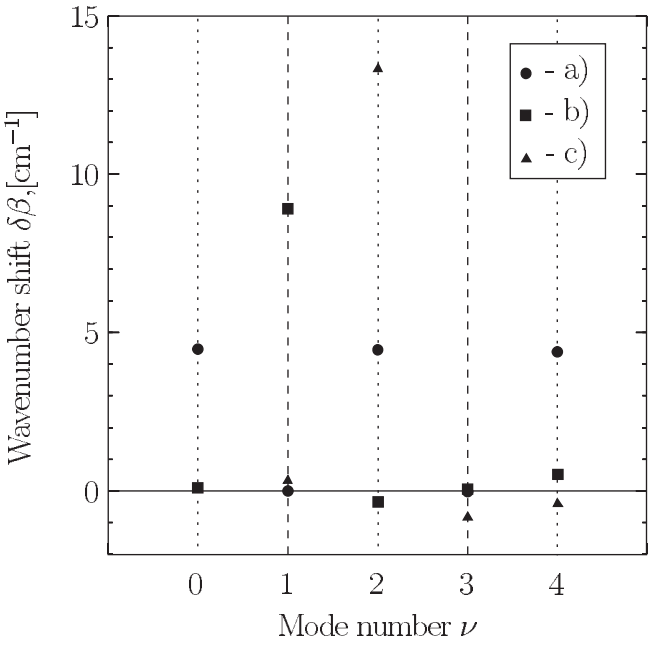

Fig. 2. Nonreciprocal phase shift for the modes of the multimode waveguide with parameters $n_{\mathrm{f}} = 2.2$, $n_{\mathrm{c}} = 1.0$, $n_{\mathrm{s}} = 1.95$, $\gamma_{\mathrm{x}} = 0.005$, $\lambda = 1.3\,\mu\mathrm{m}$, $W = 4.45\,\mu\mathrm{m}$, $h = 0.7\,\mu\mathrm{m}$. Even modes are symmetric with respect to the *xz*-plane while odd modes are antisymmetric. (a), (b) and (c) in the legend corresponds to the geometries in Fig. 1.

3. Multimode imaging

The electromagnetic field profile of a guided mode can be presented as a six-component vector

$$\mathbf{\Phi}^{v}(x,y)\exp(\mathrm{i}(\omega t-\beta^{v}z))=\begin{pmatrix}\boldsymbol{E}\\ \boldsymbol{H}\end{pmatrix}^{v}(x,y)\exp(\mathrm{i}(\omega t-\beta^{v}z)),$$

where $v=\{1,..,M\}$ indicates the number of the mode, β^{v} is a mode wavenumber, x,y are transversal coordinates and z is the propagation coordinate. The guided modes of the multimode waveguide are orthogonal and normalized with respect to the following sesquilinear form (Walker 1957)

$$(\mathbf{\Phi}^{v},\mathbf{\Phi}^{\mu})=\iint(\boldsymbol{E}^{v}\times\boldsymbol{H}^{\mu*}-\boldsymbol{H}^{v}\times\boldsymbol{E}^{\mu*})_{z}\mathrm{d}x\,\mathrm{d}y=\delta_{v\mu}. \tag{8}$$

Without loss of generality we can choose the fields $\boldsymbol{E}$ and $\boldsymbol{H}$ so that the transverse components are real, and as a result the scalar product will also be real. In this paper, we shall discuss structures with monomode waveguides as input and output ports. Apart from a remainder $\boldsymbol{\rho}$, which is orthogonal to guided modes, the mode of the input waveguide can be presented as a linear combination of the modes of the multimode waveguide

$$\Psi(x,y)=\sum_{v=1}^{M}C_{v}\mathbf{\Phi}^{v}(x,y)+\boldsymbol{\rho}(x,y). \tag{9}$$

The coefficients C_{v} in representation (9) can be found as the scalar product of the incoming field $\mathbf{\Psi}$ and the field $\mathbf{\Phi}^{v}$

$$C_{v}=(\mathbf{\Psi},\mathbf{\Phi}^{v}). \tag{10}$$

At the end of the structure, all the modes of the multimode waveguide contribute to the mode of the output waveguide. The output mode amplitude A can be calculated in the same way as at the first junction but with the phases of the modes at the end of the structure taken into account

$$A=\sum_{v=1}^{M}(\mathbf{\Psi},\mathbf{\Phi}^{v})(\mathbf{\Phi}^{v},\mathbf{\Upsilon})\exp(-\mathrm{i}\varphi_{v}). \tag{11}$$

Here $\mathbf{\Upsilon}$ is the field profile of the mode of the output waveguide, $\varphi_{v}=\beta^{v}L$ are the phases of the modes at the end of the structure $z=L$. To simplify notation, we shall introduce the abbreviation

$$(\boldsymbol{\Psi}, \boldsymbol{\Phi}^{v})(\boldsymbol{\Phi}^{v}, \boldsymbol{\Upsilon}) = w_v \exp(\mathrm{i}\vartheta_v), \tag{12}$$

where w_v and ϑ_v are the absolute value and the phase of the left-hand side of expression (12). Note that ϑ_v is either 0 or π depending on the sign of the double scalar product. Then the relative power transmitted from the input waveguide into the output waveguide is

$$P_{\text{out}} = AA^{*} = \sum_{\mu=1}^{M} \sum_{v=1}^{M} w_\mu w_v \cos(\phi_\mu - \phi_v), \tag{13}$$

where $\phi_v = \vartheta_v - \varphi_v$. Taking into account expressions (5), (6) the power output reads

$$P_{\text{out}}^{\text{f/b}} = \sum_{\mu=1}^{M} \sum_{v=1}^{M} w_\mu w_v \cos(\vartheta_\mu - \vartheta_v + (\beta_0^{\mu} - \beta_0^{v})L \pm (\delta\beta^{\mu} - \delta\beta^{v})L), \tag{14}$$

where the '+' corresponds to forward, the '−' to backward propagation. In structures with equal nonreciprocal phase shifts for all excited modes there is no difference in power output for forward and backward directions so we need at least one mode with a different nonreciprocal phase shift $\delta\beta$.

We considered only forward propagating guided modes, backward propagating guided modes caused by reflections in the junction will degrade the device performance. According to Öz *et al.* (1998), the power loss due to reflection into backward propagating guided modes is approximately 3% of all the losses. The power P_{rfl} reflected into the guided modes can be estimated as

$$10 \log_{10} \frac{P_{\text{rfl}}}{P_{\text{in}}} \approx -25\,\text{dB}. \tag{15}$$

Smooth transitions from monomode to multimode waveguide will improve the isolation.

4. Isolator with off-center input

The structure presented in Fig. 3 with geometrical parameters from Table 1 supports only two modes, one symmetric and one antisymmetric. The relative power transmitted into port B can be written in the form

$$P_{\text{out}} = w_s^2 + w_a^2 + 2w_s w_a \cos(\phi_s - \phi_a). \tag{16}$$

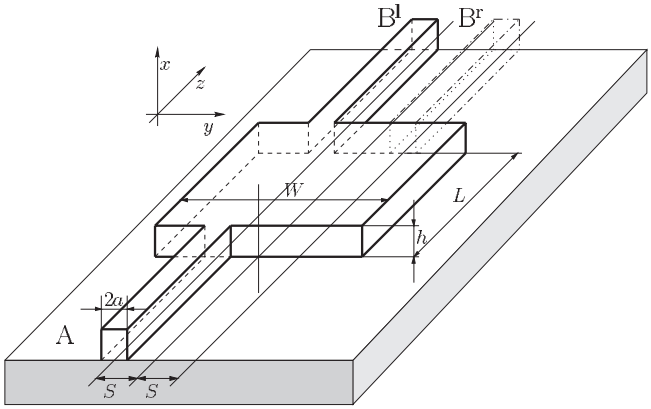

Fig. 3. Isolator with input shifted from the center of the multimode waveguide. There are two possible configurations: the input and output waveguides form a line (port B^{l}); the input and output waveguides are displaced (port B^{r}).

The output power can be zero only when $w_a = w_s$. This may be achieved in a structure with in- and outlets displaced from the central position. The conditions for the output power to be minimal or maximal read

$$P_{\mathrm{out}}^{\mathrm{min}}: \quad \cos(\phi_s - \phi_a) = -1, \tag{17}$$

$$P_{\mathrm{out}}^{\mathrm{max}}: \quad \cos(\phi_s - \phi_a) = 1. \tag{18}$$

For this, the wavenumbers of the structure where $P_{\mathrm{out}}^{\mathrm{f}} = P_{\mathrm{out}}^{\mathrm{max}}$ and $P_{\mathrm{out}}^{\mathrm{b}} = P_{\mathrm{out}}^{\mathrm{min}}$ must fulfill the condition

$$\frac{\beta_{\mathrm{f}}^s - \beta_{\mathrm{f}}^a}{\beta_{\mathrm{b}}^s - \beta_{\mathrm{b}}^a} = \frac{2\pi n + \vartheta_s - \vartheta_a}{2\pi m + \pi + \vartheta_s - \vartheta_a}, \tag{19}$$

Table 1. Parameters for the nonreciprocal multimode imaging devices. The material parameters are in all cases $n_{\mathrm{c}} = 1.0$, $n_{\mathrm{f}} = 2.2$, $n_{\mathrm{s}} = 1.95$, $\gamma_{\mathrm{x}} = 0.005$ and $\lambda = 1.3\,\mu\mathrm{m}$. Line 'Geom.' indicates the geometry of the nonreciprocal phase shifter according to Fig. 1

	Isolator		Circulator	
	Noncentral	Central	I	II
Geom.	b	c	a	a
h	0.7 μm	0.7 μm	0.7 μm	0.7 μm
a	0.37 μm	0.5 μm	0.5 μm	0.5 μm
W	1.59 μm	4.175 μm	4.45 μm	4.45 μm
S	1.1 μm	0.0 μm	1.1 μm	1.1 μm
L	730.24 μm	816.33 μm	3530.5 μm	3658.5 μm
$A \to B$	−2 dB	−5 dB	−30 dB	−3 dB
$A \to D$	–	–	−3 dB	−30 dB
$B \to A$	$-\infty$	−85 dB	−3 dB	−30 dB
$B \to C$	–	–	−30 dB	−3 dB

where n and m are integers. The length of the multimode waveguide can be found from the expression

$$L = \frac{\pi(2n - 2m - 1)}{2|\delta\beta^s - \delta\beta^a|}. \tag{20}$$

We require $|\delta\beta^s - \delta\beta^a|$ as large as possible so the four-domain structure is the best choice for the phase shifter, but the two-domain structure may serve as well. Fig. 4 shows the dependence of the output power in forward direction for geometries where the output power in backward direction vanishes. Indices l(eft) and r(ight) indicate the displacement of the output waveguide. It is possible to achieve reasonably good performance in the structure with $P^{\mathrm{b}}_{\mathrm{out}} = 0$ and a device length close to the value $L_{\mathrm{opt}} = \pi/2|\delta\beta^s - \delta\beta^a|$.

5. Isolator with centered input

In a structure with centered input (Fig. 5) only symmetric modes are excited. To make light vanishing completely at a certain point we need at least three symmetric modes because there is no geometry with equal overlap to

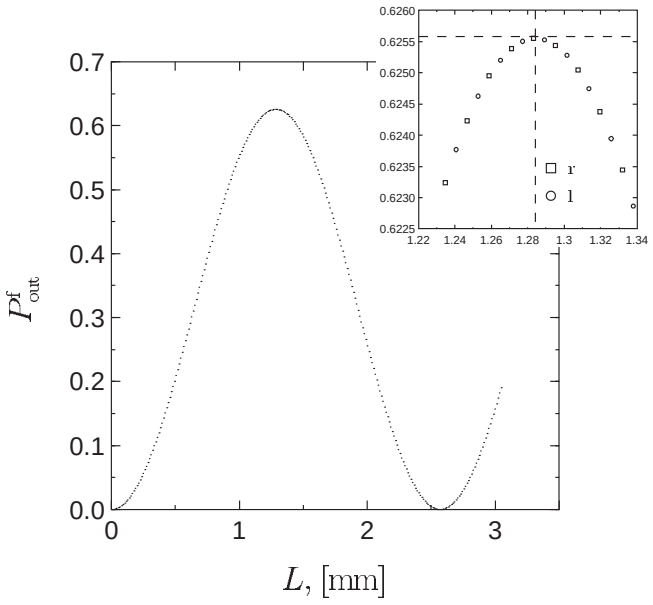

Fig. 4. Points representing power output in forward direction for structures that block the light in backward direction. Structure parameters: $n_{\mathrm{f}} = 2.2$, $n_{\mathrm{c}} = 1.0$, $n_{\mathrm{s}} = 1.95$, $\gamma_{\mathrm{x}} = 0.005$, $\lambda = 1.3\,\mu\mathrm{m}$, $W = 1.59\,\mu\mathrm{m}$, $a = 0.37\,\mu\mathrm{m}$, $S = 1.1\,\mu\mathrm{m}$, $h = 0.7\,\mu\mathrm{m}$ and domain configuration of Fig. 1(a).

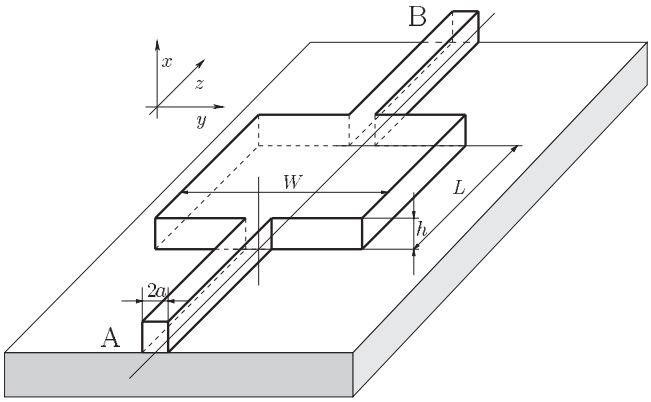

Fig. 5. Isolator with central input.

the first and second symmetric modes. From (13) and Fig. 2 we see that the only suitable phase shifter for the symmetric isolator is the six-domain structure. The two- and four-domain structures exhibit no forward/backward asymmetry since the nonreciprocal phase shifts of symmetric modes are equal in these structures. The mode amplitude in the output waveguide (11) can be represented as a sum of vectors in the complex plane with lengths w_0, w_2 and w_4 and angles equal to the phases of the modes at the end of the structure in Fig. 6. Using this simple geometrical picture, we may write down a system of equations for a structure with maximal power transmission in forward direction while blocking the backward direction completely:

$$\begin{aligned}
&\beta_{\mathrm{f}}^2 L - \beta_{\mathrm{f}}^0 L = 2\pi k \\
&\beta_{\mathrm{f}}^4 L - \beta_{\mathrm{f}}^0 L = 2\pi l \\
&w_0 + w_2 \cos(\beta_{\mathrm{b}}^2 L - \beta_{\mathrm{b}}^0 L) + w_4 \cos(\beta_{\mathrm{b}}^4 L - \beta_{\mathrm{b}}^0 L) = 0 \\
&w_2 \sin(\beta_{\mathrm{b}}^2 L - \beta_{\mathrm{b}}^0 L) + w_4 \sin(\beta_{\mathrm{b}}^4 L - \beta_{\mathrm{b}}^0 L) = 0.
\end{aligned} \tag{21}$$

$\beta_{\mathrm{f,b}}^{0,2,4}$ are the wavenumbers of forward and backward propagating symmetric modes, k and l are integers. System (21) depends on four geometrical parameters W, a, h and L which can be adjusted to solve the system of four equations. High isolation is also achieved by fulfilling the second pair of equations (blocking conditions) only while keeping the transmission at a reasonable high level. As can be seen from Fig. 6, the output power vanishes when the vectors form a triangle. Using this geometrical interpretation, a condition for the mode wavenumbers for completely destructive interference for backward propagating light can be derived:

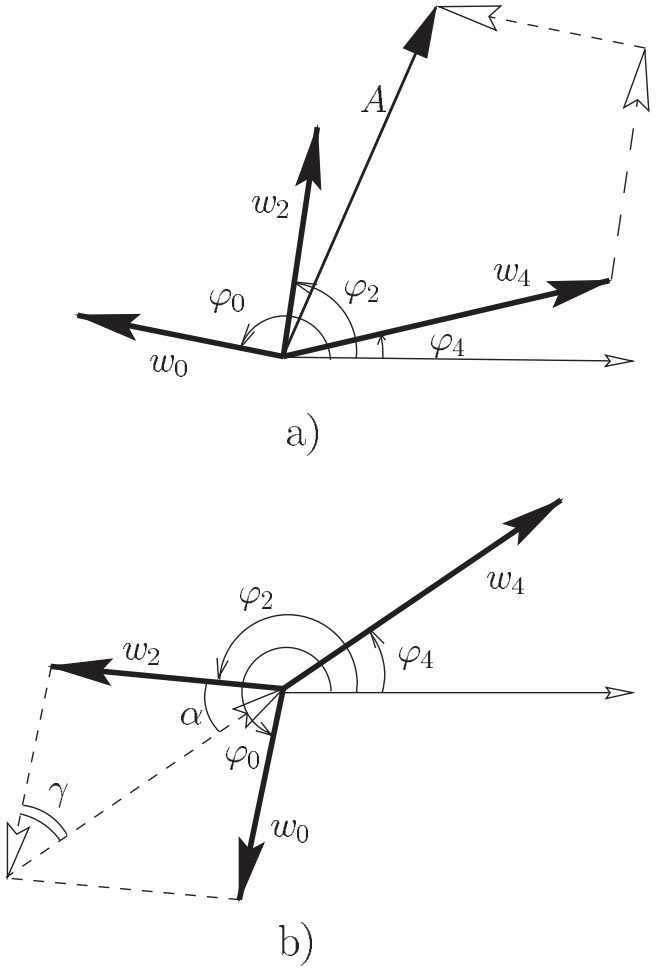

Fig. 6. The amplitude A of the output mode (see expression (11)) can be represented as a sum of vectors w_0, w_2 and w_4: (a) $|A| \neq 0$, (b) $|A| = 0$.

$$\frac{(\beta_b^0 - \beta_b^2)}{(\beta_b^0 - \beta_b^4)} = \frac{\pi(2n+1) + \alpha}{\pi(2m+1) + \gamma}, \tag{22}$$

the angles α and γ can be worked out using the cosine theorem. In a structure where condition (22) is satisfied, the length of the multimode waveguide is given by the expression

$$L = \frac{\pi(2n+1) + \alpha}{(\beta_b^0 - \beta_b^2)}. \tag{23}$$

The parameters of such a structure and its performance are presented in Table 1.

6. Circulator

Fig. 7 illustrates the power transmission cycle of a four port circulator. Light entering at port A leaves the device at port B while light entering at B is transferred to port C. This behavior can be reproduced using a multimode waveguide with four monomode connectors as shown in Fig. 8. The separation S must be large enough to avoid crosstalk between neighboring monomode waveguides. This establishes a lower limit to the width of the multimode waveguide W, and as a result we have to cope with a large number of modes both symmetric and antisymmetric, and an analytical approach is rather complicated. Fig. 9 shows the performance of the circulator with parameters presented in Table 1. Column I refers to a structure where

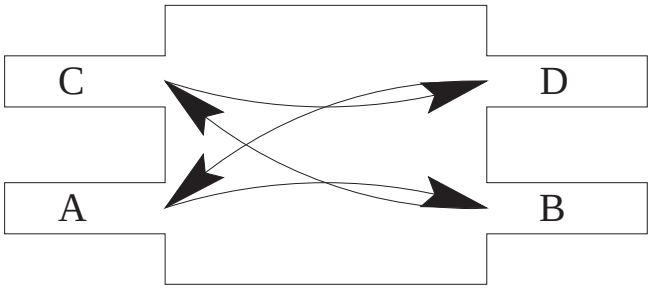

Fig. 7. Circulator scheme.

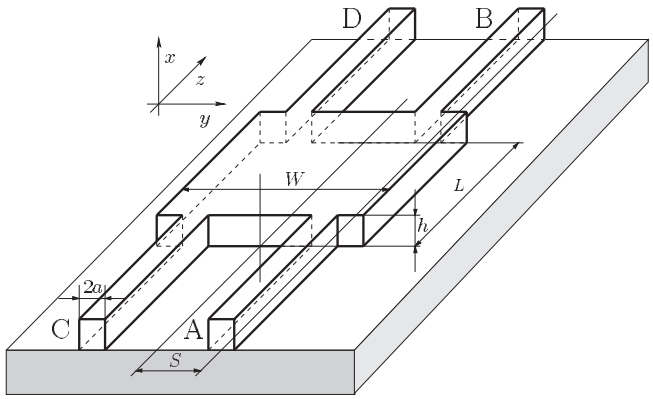

Fig. 8. Circulator based on multimode imaging.

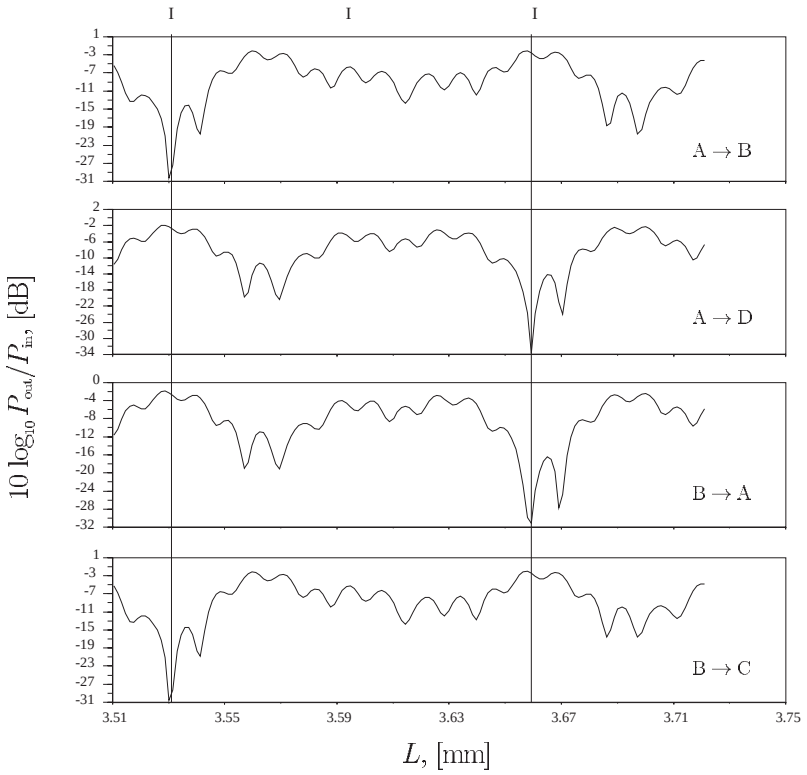

Fig. 9. Circulator performance. Lines I and II correspond to the devices of columns I and II in Table 1.

channels B to A, A to D, D to C and C to B are open. Column II describes a slightly longer structure where A to B, B to C, C to D and D to A are open. Put otherwise, the two circulators operate in opposite routing directions.

7. Conclusions

Two new concepts for an integrated optical isolator and a new concept for a four port circulator are presented. The tolerance requirements on geometric parameters are as strict as for all other integrated optical isolators (Zhuromskyy *et al.* 1999). However, the proposed devices are much simpler to fabricate and tune. To realize an optical isolator, the structures 1(a) and 1(b) with non-central input are best suited, because only two interfering optical modes are required. In contrast to an isolator with central input utilizing structure 1(c), three modes are necessary. To realize a circulator, all structures of Fig. 1 can be applied, in each case five optical modes are required. However, structure (a) is best because it induces a nonreciprocal phase shift

for three modes leading to higher power transition, the others only for one mode.

Acknowledgement

Financial support by Deutsche Forschungsgemeinschaft (Graduiertenkolleg *Mikrostruktur oxidischer Kristalle* and Sonderforschungsbereich *Oxidische Kristalle für elektro- und magnetooptische Anwendungen*) is gratefully acknowledged.

References

Ando, K., T. Okoshi and N. Koshizuka. *Appl. Phys. Lett.* **53** 4, 1988.
Auracher, F. and H.H. Witte. *Opt. Commun.* **13** 435, 1975.
Bahlmann, N., M. Lohmeyer, M. Wallenhorst, H. Dötsch and P. Hertel. *Opt. Quant. Electr.* **30** 323, 1998.
Bahlmann, N., M. Lohmeyer, O. Zhuromskyy, H. Dötsch and P. Hertel. *Opt. Commun.* **161** 330, 1999.
Hemme, H., H. Dötsch and P. Hertel. *Appl. Opt* **29** 2741, 1990.
Jenkins, R.M., J.M. Heaton, D.R. Wight, J.T. Parker, J.C.H. Birbeck and G.W. Smith. *Appl. Phys. Lett.* **64** 684, 1994.
Krauss, T.F., R.M. De La Rue and P.J.R. Laybourn. *J. Lightw. Technol.* **13** 1500, 1995.
Lohmeyer, M. *Opt. Quant. Electr.* **29** 907, 1997.
Lohmeyer, M. *Opt. Quant. Elect.* **30** 385, 1998.
Lohmeyer, M., M. Shamonin, N. Bahlmann, P. Hertel and H. Dötsch. Radiatively coupled waveguide concept for an integrated magneto-optic circulator. In *High-Density Magnetic Recording and Integrated Magneto-Optics: Materials and Devices*, eds. K. Rubin, J.A. Bain, T. Nolan, D. Bogy, B.J.H. Stadler, M. Levy, J.P. Lorenzo, M. Mansuripur, Y. Okamura and R. Wolfe, Vol. 517, MRS Symposium Proceedings Series, 519–524, 1998.
Lohmeyer, M., N. Bahlmann, O. Zhuromskyy, H. Dötsch and P. Hertel. *J. Lightw. Technol.* **17** 2605, 1999.
Okamura, Y., T. Negami and S. Yamamoto. *Appl. Opt.* **23** 1886, 1984.
Öz, M. and R.R. Krchnavek. *J. Lightw. Technol.* **16** 2451, 1998.
Popkov, A.F., M. Fehndrich, M. Lohmeyer and H. Dötsch. *Appl. Phys. Lett.* **72** 2508, 1998.
Shintaku, T. *Appl. Phys. Lett.* **66** 2789, 1995.
Soldano, L.B. and E.C.M. Pennings. *J. Lightw. Technol.* **13** 615, 1995.
Walker, L.R. *J. Appl. Phys.* **28** 377, 1957.
Wallenhorst, M., M. Niemöller, H. Dötsch, P. Hertel, R. Gerhardt and B. Gather. *J. Appl. Phys.* **77** 2902, 1995.
Wolfe, R., J.R. Dillon, R.A. Liberman and V.J. Fratello. *Appl. Phys. Lett.* **57** 960, 1990.
Yamamoto, S., Y. Okamura and T. Makimoto. *IEEE J. Quant. Electr.* **12** 764, 1976.
Zhuromskyy, O., M. Lohmeyer, N. Bahlmann, H. Dötsch and P. Hertel. *J. Lightw. Technol.* **17** 1200, 1999.